Available online at www.sciencedirect.com
ScienceDirect
Polymer 48 (2007) 363–370
polymer
www.elsevier.com/locate/polymer

Ultradrawing above the static melting temperature of ultra-high molecular weight isotactic poly(1-butene) having low ductility in the crystalline state

Daisuke Sawai*, Takashi Anyashiki, Koh Nakamura, Nobumi Hisada, Takuro Ono, Tetsuo Kanamoto

Department of Applied Chemistry, Tokyo University of Science, Kagurazaka, Shinjuku-ku, Tokyo 162-8601, Japan

Received 21 June 2006; received in revised form 9 November 2006; accepted 12 November 2006
Available online 30 November 2006

Abstract

Ultra-high molecular weight isotactic poly(1-butene) (UHMW-PB1) melt-grown crystal (MGC) films were drawn using the PIN drawing technique. Although the UHMW-PB1 MGC films had poor ductility in the crystalline state, they were ultradrawable in the molten state above the static melting temperature (T_m). The drawability of the MGC films was strongly influenced by the draw temperature, the sample thickness, and the contact time between the metal heater and sample, and it increased with decreasing sample thickness. The maximum draw ratio (DR_{max}) was nearly constant when the sample thickness was less than 100 μm at a given draw temperature. The contact time between the metal heater and sample needed to draw continuously in the molten state was at least 0.1 s. The ductility increased rapidly above 130 °C, reaching a maximum at 200 °C, and decreased at higher temperatures. A DR_{max} of 170 was achieved at 200 °C under optimum conditions. The efficiency of the drawing, based on the Herman crystalline orientation function (f_c) and tensile properties versus DR, was lower for films drawn at higher temperatures. The highest f_c of 0.996, tensile modulus of 14 GPa, and strength of 900 MPa were obtained by ultradrawing with DR = 50 at 155 °C. This modulus corresponded to 58% of the X-ray crystal modulus (24 GPa), whereas the modulus of PB1 films drawn in the crystalline state corresponded to only 12–13% (3 GPa) of the theoretical crystal modulus.

Keywords: Ultra-high molecular weight poly(1-butene); Melt drawing; Mechanical properties

1. Introduction

Isotactic poly(1-butene) (PB1) exhibits four crystal modifications depending on the formation conditions [1]: phase I, twinned hexagonal with a 3_1 helix [2]; phase I′, untwined hexagonal with a 3_1 helix; phase II, tetragonal with a 11_3 helix [3]; and phase III, orthorhombic with a 4_1 helix [4]. PB1 exhibits transient polymorphic behavior upon cooling from the melt state at atmospheric pressure [5–9]. PB1 first crystallizes into the unstable phase II crystals from the melt state. The unstable phase II crystals can transform into the stable hexagonal phase I crystals. The kinetics of this phase transformation is known to be influenced by strain [10,11], pressure [12], and temperature [7]. Phase III and I′ crystals have been found to form upon crystallization from solution [3,13] depending on the solvent, concentration, and the crystallization temperature. Phase III and I′ crystals transform to oriented phase II crystals upon tensile drawing [14] even below the static melting temperature, T_m. Moreover, the drawing of PB1 proceeds either through melting/recrystallization or in the crystalline state, depending on the draw technique, temperature, and the crystal form of the starting sample [14].

The ductility of polymers is affected by several parameters which are related to the chemical structure, initial morphology, and drawing conditions. Generally, polymers with high chain rigidity and strong intermolecular interactions have low ductility [15]. The drawability of a given polymer is also strongly affected by other variables, including chain entanglement density [16]

* Corresponding author.
E-mail address: dsawai@rs.kagu.tus.ac.jp (D. Sawai).

0032-3861/$ - see front matter © 2006 Elsevier Ltd. All rights reserved.
doi:10.1016/j.polymer.2006.11.020

and sample molecular weight [17–19]. The draw technique and conditions are also crucial [20]. It has also been shown that polymer ductility increases above the crystalline relaxation or reversible crystal/crystal transition temperature [21–25]. Only a few polymers have been successfully superdrawn to the limit where the tensile moduli approached the X-ray crystal moduli. These polymers include ultra-high molecular weight (UHMW) polyethylene (UHMW-PE) [26], UHMW polypropylene (UHMW-PP) [21], UHMW polytetrafluoroethylene (UHMW-PTFE) [27], UHMW polyacrylonitrile (UHMW-PAN) [18], and UHMW poly(4-methyl-1-pentene) (P4M1P) [22]. Superdrawing was achieved by drawing from low entangled states. On the other hand, despite the continuing and extensive attempts to achieve an extreme draw with a number of polymers, high drawability has not been achieved for poly(ethylene terephthalate) and polyamides, which are some of the most important industrial polymers. With these polymers, the moduli were 5–30% of the X-ray theoretical crystal moduli. The low drawability was thought to be due to lack of a crystal/crystal transition and/or crystal dispersion in which molecular mobility was activated; such transitions and dispersion did not occur below the T_m [24]. Therefore, a new drawing method for transforming low-ductility polymers into high-performance polymers is required.

Isotactic poly(1-butene) also had low drawability in the crystalline state, even when UHMW-PB1 solution-grown crystal mats prepared from a dilute solution [28] were used, although PB1 has a chemical structure similar to those of PE, PP, and P4M1P, which have been successfully superdrawn [21,22,26]. This may be due to the fact that the crystal modifications of PB1 did not undergo crystalline relaxation. The maximum reported tensile modulus for PB1 was 1–3 GPa [28,29], which corresponds to about 5–13% of the theoretical crystal modulus (24 GPa) reported by Sakurada and Kaji [30]. However, those of PE, PP, and P4M1P were 80–90%.

Most drawing techniques are carried out below T_m because drawing in the crystalline state keeps the degree of entanglement low and produces the best mechanical properties. Recently, however, our group has reported that UHMW-PTFE reactor powder films can be drawn by the PIN drawing technique above T_m under controlled conditions [31], whereas PIN drawing below T_m resulted in lower drawability due to the excessive molecular mobility and less entanglement. The draw was effective above T_m because the effective entanglement was higher and there was less draw stress above T_m than in the crystalline state. The UHMW-PTFE samples prepared above T_m had a high tensile modulus and were highly oriented.

We have also systematically improved the method of drawing UHMW-PE from melt by optimizing the sample molecular weight, thermal history, initial morphology, and drawing conditions [32,33]. As a result of the optimization, high drawability above T_m was achieved for UHMW-PE melt-crystallized films having a high entanglement density, although these films had poor ductility in the crystalline state [16,32]. These highly drawn samples had better mechanical properties than those of samples drawn in the crystalline state. This suggests that the ductility of the sample, which was initially low, increased, depending on the initial morphology, sample molecular weight, thermal history, and drawing conditions. Similar results may also be possible for other polymers. Recently, the deformation and the formation of structure in samples of PB1, which has poor ductility in the crystalline state, above T_m have been reported [34,35].

In this article, we report the ultradrawing and the formation of oriented structure using the PIN draw technique above T_m of UHMW-PB1 MGC films, which have low ductility below T_m. We also report the mechanical properties and chain orientation of the resultant samples drawn by using the PIN drawing method above T_m.

2. Experimental section

2.1. Samples

The UHMW-PB1 used in this work was M801P, supplied by Mitsui Chemicals Co. Ltd. Its viscosity-average molecular weight (M_v) was 2.6×10^6, and it had ^{13}C NMR isotactic pentad fraction of 93.9%. Melt-grown crystal (MGC) film samples were prepared by compression molding at a press temperature (T_p) of 180 °C and a pressure of 2.5 MPa for 5 min, followed by slow cooling to room temperature.

2.2. Drawing

The MGC films were drawn by using the PIN drawing apparatus shown in Fig. 1. The MGC films were cut into strips, $60 \times 1–3 \times 0.07–0.5$ mm^3. Both ends of the samples were fixed onto Kevlar fibers, and the samples were attached via the Kevlar fibers to the PIN drawing apparatus. A small portion (2 mm) of these strips was heated by contacting it with the surface of a heated metal cylinder kept at a constant temperature (drawing temperature, $T_d = 30–220$ °C), and the strips were then quickly drawn to the desired draw ratio at a constant throughput rate (5–180 cm/min) and take-up velocity (30–10,000 cm/min). The drawing was started 0.1 s after contact between the sample and the metal heater by activating a solenoid. During the drawing, the contact area of the strip was continuously moved from one end to the other at a constant throughput rate, and successive drawn samples were obtained. The draw stress was detected by using a load cell. The effects of the sample thickness and throughput rate on drawability by PIN drawing are discussed later.

2.3. Characterization

WAXD patterns were recorded using a flat-plate camera and diffractometer scans. Photographs were obtained with Cu Kα radiation generated at 40 kV and 25 mA on a Rigaku Geigerflex RAD-3A and monochromatized by using a graphite crystal. The diffraction profiles were recorded with Ni-filtered Cu Kα radiation generated at 50 kV and 300 mA on a Rigaku Ultrax18 equipped with a diffractometer and a pulse height discriminator. Crystalline chain orientation was evaluated by the Herman orientation function, f_c [35]. The f_c was evaluated

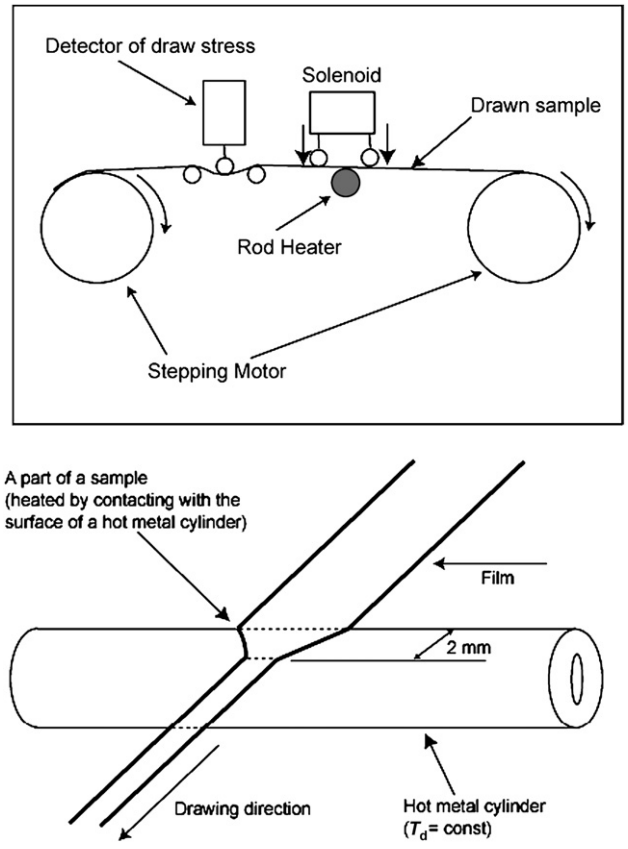

Fig. 1. A schematic drawing of the PIN drawing apparatus.

using the (110) index of phase I crystals, assuming fiber symmetry, as reported by Oda et al. [36]. The azimuthal intensity distribution was recorded at step scan intervals of 0.1° in the azimuthal angle using a Rigaku fiber specimen holder with a first collimator with a diameter of 0.5 mm and a receiving slit of 1.8° (2θ direction) × 0.3° (azimuthal direction).

Optical microscopy (OM) observations were made with an Olympus optical microscope, Model BHSP.

The tensile modulus and strength along the fiber axis were measured at room temperature and strain rates of 1×10^{-3} s^{-1} and 1×10^{-2} s^{-1}, respectively, on an Orientec Tensilon tensile tester.

3. Results and discussion

The PB1 MGC films transformed from phase II to I on physical aging at room temperature. First, the time dependence of the crystal transformation from phase II to I of the UHMW-PB1 MGC film was examined because it was necessary to use MGC films with the same crystalline state in the PIN drawing. Fig. 2 shows the effect of aging time at room temperature on the WAXD profiles. In the WAXD profiles of the sample that were aged for 1 h at room temperature, a mixture of crystal forms, corresponding to phase I and II crystal reflections, was observed. The peak intensities due to phase I crystals in the WAXD profiles increased with increasing aging time at room temperature, and the reflection due to phase II crystals disappeared after 5 days. Therefore, the sample that was aged for

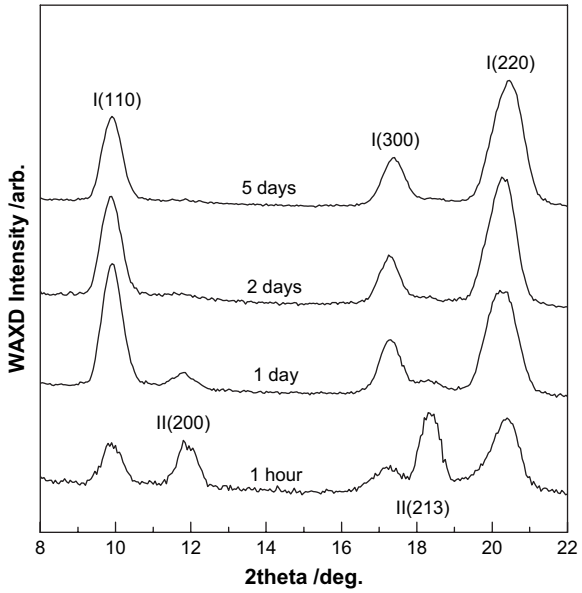

Fig. 2. WAXD diffraction profiles for MGC films versus aging time at room temperature.

5 days was chosen as the starting material for PIN drawing. The peak melting temperature and onset melting temperature of the phase I crystals estimated by DSC measurements were 122 °C and 131 °C, respectively.

Fig. 3 shows the dependence of the sample thickness on the maximum achieved draw ratio (DR_{max}). The PIN drawing temperatures were 155 °C and 180 °C, which are above T_m of the MGC films. The throughput rate was constant at 20 cm/min. At a given temperature, the DR_{max} significantly decreased with increasing sample thickness. The samples that had a thickness greater than 400 μm at 155 °C and 600 μm at 180 °C could not be drawn by using the PIN drawing method. The large

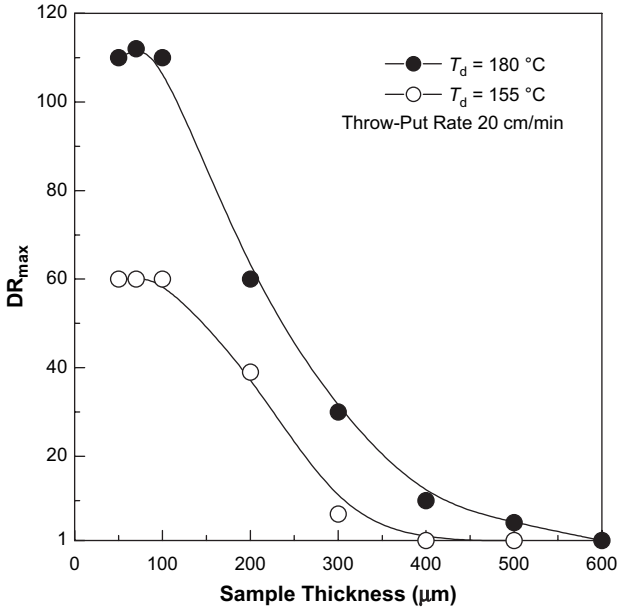

Fig. 3. DR_{max} of the MGC films as a function of sample thickness for PIN drawing at T_d = 155 °C and 180 °C. The throughput rate was constant at 20 cm/min.

thickness was the main reason that these samples did not completely melt in a short time, because the samples were heated by a metal heater from below. By decreasing the sample thickness, the drawability increased, and the drawability was constant for sample thicknesses below 100 μm. The DR_{max} values were 58 at $T_d = 155$ °C and 110 at $T_d = 180$ °C. Thus, samples with a thickness of 100 μm were used in the PIN drawing.

Fig. 4 shows the dependence of throughput rate on DR_{max}. The T_ds were 155 °C and 180 °C. DR_{max} increased as the throughput rate decreased. The drawability only had a slight dependence on the throughput rate in the range of 5–120 cm/min independent of draw temperature, for example, $DR_{max} = 100–112$ at $T_d = 180$ °C and $DR_{max} = 52–59$ at $T_d = 155$ °C. For higher throughput rates, the drawability decreased rapidly with the throughput rate. A throughput rate ranging from 5 to 180 cm/min corresponded to a contact time between the sample and the metal heater of 0.06–2.4 s. When the drawability decreased rapidly, the contact time corresponded to less than 0.08 s (throughput rate = 150 cm/min). On the other hand, continuous PIN drawing above T_m was not possible when the contact time between sample and the metal heater was less than 0.1 s. These results suggest that the contact time between the PB1 MGC films with a thickness of 100 μm and the metal heater needs to be at least 0.1 s to draw continuously by the PIN drawing method in the molten state. Based on an experiment discussed later, the throughput rate was set to 20 cm/min for the PIN drawing.

Fig. 5 shows DR_{max} of the UHMW-PB1 MGC films as a function of PIN T_d (30–220 °C). Below $T_d = 100$ °C, the drawability decreased. Above $T_d = 100$ °C, the drawability increased with increasing T_d, reaching a maximum at a certain T_d. In particular, the drawability increased rapidly with T_d above T_m. The drawability was highest with DR = 170 at $T_d = 200$ °C. High drawability was achieved by using the

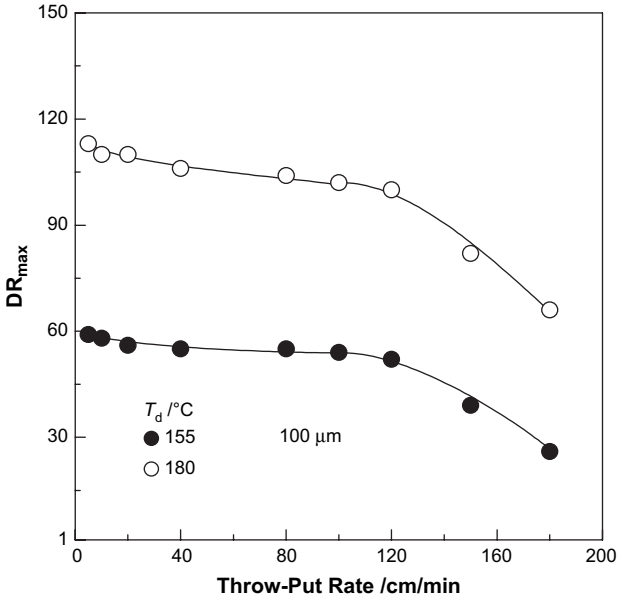

Fig. 4. DR_{max} of the MGC films as a function of throughput rate during PIN drawing at $T_d = 155$ °C and 180 °C. The sample thickness was constant at 100 μm.

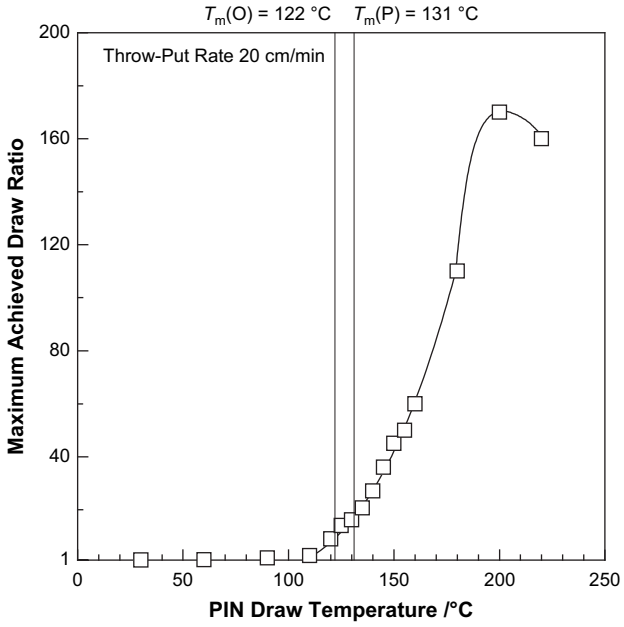

Fig. 5. Maximum achieved DR of the MGC films as a function of the PIN drawing temperature, T_d.

PIN drawing method above T_m because the draw stress above T_m was significantly lower than that in the crystalline state (2–6 MPa versus 20–35 MPa) since UHMW-PB1 did not undergo crystalline relaxation. Therefore, disentanglement and/or slippage of the chain molecules occurred only moderately during the melt draw. At higher T_d, the ductility decreased rapidly with increasing T_d. We believe that continuous PIN drawing was not possible at $T_d = 220$ °C because the propagation of draw stress to the chain molecule was insufficient due to high mobility.

Fig. 6 shows WAXD photographs of the DR_{max} samples of the UMW-PB1 MGC films at a given temperature. Oriented phase II crystals appeared during PIN draw when the PIN draw was performed above T_m ($T_d \geq 130$ °C). Therefore, WAXD patterns of oriented phase I samples left to stand for one week after PIN drawing was taken at room temperature. In the case of drawing at $T_d = 110$ °C in the crystalline state, the chain orientation was lower due to the DR_{max} of 2.7. The reflections became gradually sharper, and the intensity distribution concentrated on the equator and off-equator with increasing T_d, even during PIN drawing above T_m. The changes in the WAXD patterns with T_d indicate that the chains were progressively oriented and crystallized along the drawing direction. The sample with the highest orientation was obtained by PIN drawing at $T_d = 155$ °C. The spotty reflection indicates a high chain orientation along the draw axis. The details were estimated using f_c.

The crystalline chain orientation was evaluated using f_c, determined by WAXD [37]. The f_c function was calculated from the (110) reflection of phase I crystals, assuming fiber symmetry [36]. Fig. 7 shows f_c versus DR for PIN drawing at various T_d. The f_c for each film increased rapidly with DR in the lower temperature range and reached $f_c > 0.98$ at DR = 20 in all T_d regions, except for the drawing at T_d's ≤ 120 °C in

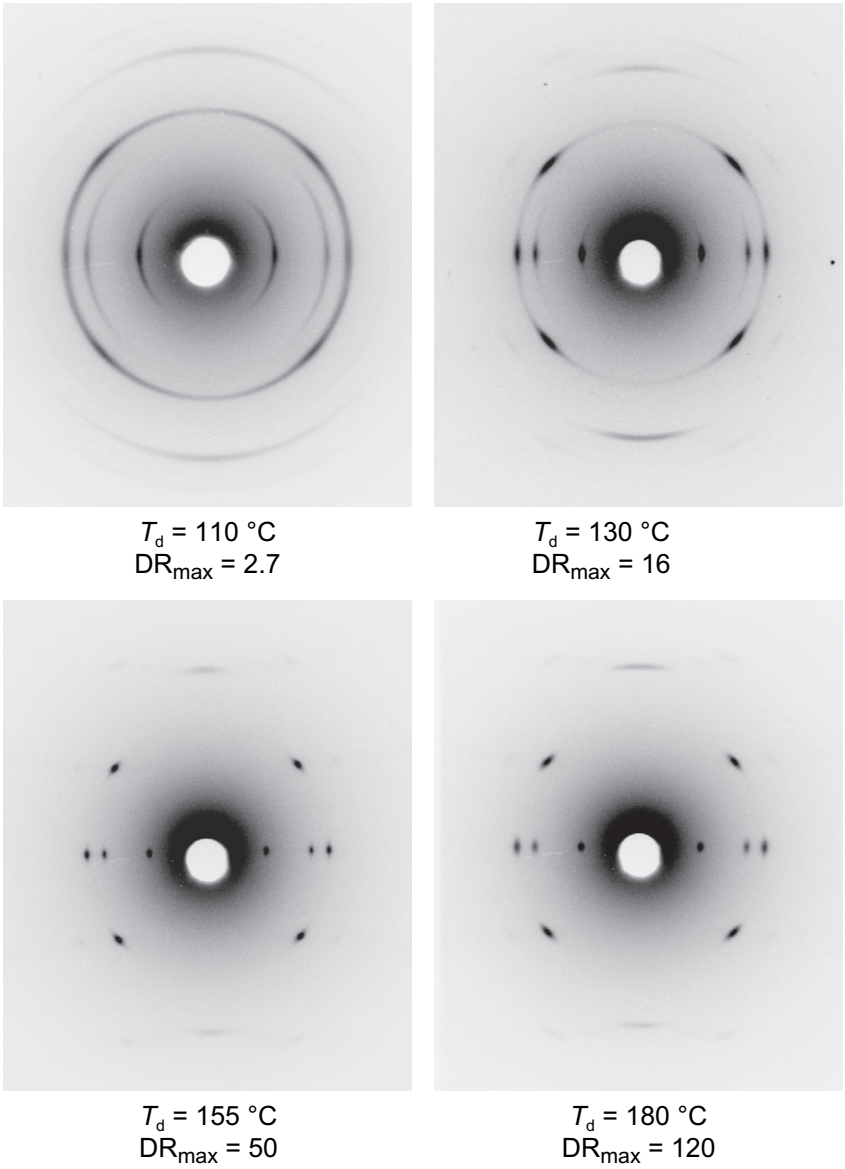

Fig. 6. WAXD photographs of films drawn at different drawing temperatures (T_d ranging from 110 °C to 180 °C). The DR_{max} values are also shown.

the crystalline state. The degree of chain orientation in the lower DR region was higher for the samples drawn at a lower T_d. In a higher DR region, it increased slowly with DR, independent of T_d. The f_c reached a maximum value of 0.996 at DR = 50 and T_d = 155 °C because the drawability increased with T_d. At higher T_d, the maximum f_c was slightly lower (0.992–0.994) although the ductility was higher than that at T_d = 155 °C. These results agreed with the relationship between the maximum achieved mechanical properties and draw temperature, as mentioned later. The f_c values achieved from the PIN drawing above T_m were significantly higher than those of the PB1 tapes (about 0.97) drawn in the crystalline state [29]. These high f_c values indicate nearly perfect chain orientation in the highly drawn samples, even though the samples were melt drawn.

PB1 exhibits four crystal modifications and various crystal transformations depending on the initial crystal modification and sample preparation conditions. Therefore, by tracing the crystal form and crystal transformation of the drawn samples, deformation during PIN drawing proceeds either through melting, partial melting, or in the crystalline state. The crystal form after PIN drawing was estimated from WAXD measurements at room temperature. WAXD measurements were performed as soon as possible after PIN drawing because phase II crystals transformed into phase I crystals at room temperature, as shown in Fig. 2. Fig. 8 shows the WAXD profiles on equator for a range of draw temperatures of the DR = 10 samples left to stand for 5 min after PIN drawing and for a series of aged samples with DR = 10 drawn at T_d = 155 °C. Only phase I crystals were observed by WAXD in the sample drawn at T_d = 120 °C. This indicates that deformation during the PIN drawing at T_d = 120 °C proceeded in the crystalline state. The crystal forms of the sample drawn at T_d = 130 °C were a mixture of phase I and II crystals. The crystal forms of samples drawn at T_d = 140 °C and 155 °C exhibited only phase II crystals after 10 min. These

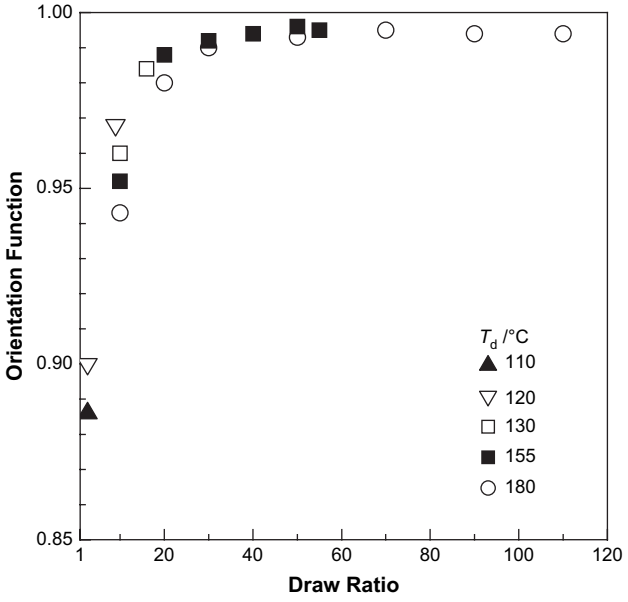

Fig. 7. Orientation function, f_c, versus DR for PIN drawing of MGC films at $T_d = 110$ °C (▲), 120 °C (▽), 130 °C (□), 155 °C (■) and 180 °C (○).

results suggest that the deformation during the PIN drawing proceeded through a partial melt state at $T_d = 130$ °C and in the molten state at $T_d \geq 140$ °C. The peak melting temperature and onset melting temperature of the initial PB1 MGC films with phase I crystals, estimated by DSC measurements, were 131 °C and 122 °C, respectively. The time dependences of the crystal transformation from oriented phase II to I samples drawn at $T_d = 155$ °C were also measured by WAXD on the equator. The crystal transformation of the DR = 10 sample drawn at $T_d = 155$ °C completed after 1 day, whereas initial MGC films took 5 days to transform from phase II to I. This may be due to the fact that the kinetics of this crystal transformation was accelerated by the stress remaining in the drawn sample [10,11], and the crystal transformation to phase I proceeded easily from the film surface [38] because the surface area of the sample was increased by the drawing. Thus, deformation during the PIN drawing above $T_d = 140$ °C proceeded through melting.

Fig. 9 shows the room temperature tensile modulus versus DR for PIN drawing of MGC films for $T_d = 110$–180 °C. The modulus of the drawn films increased rapidly with DR in all T_d ranges, and the efficiency of draw increased with decreasing T_d. In the case of films drawn at $T_d = 120$ °C, the maximum achieved modulus was low (3 GPa) because of the low DR_{max} achieved in the crystalline state. When the UHMW-PB1 films were PIN drawn above T_m, the tensile modulus increased with DR more gently than that for drawing in the crystalline state. The maximum modulus of the drawn film was 14 GPa at DR = 50 and $T_d = 155$ °C. This modulus corresponded to 58% of the X-ray crystal modulus (24 GPa), whereas the modulus of PB1 films drawn in the crystalline state corresponded to 12–13% of the theoretical crystal modulus. The maximum achieved modulus of 14 GPa is four to five times higher than that of the PB1 films (3 GPa) drawn in the solid state. At high T_d ($T_d = 180$ °C), for example, although the modulus increased with DR, the maximum achievable modulus was lower than that of the sample drawn at $T_d = 155$ °C. This may be due to the fact that chain extension, orientation, and crystallization during the melt drawing did not significantly occur at higher T_d. In addition, in higher DR region, its decrease is likely related to the formation of defects that were observed using OM.

Only a few polymers have been successfully superdrawn to the limit of their tensile moduli, that is, approaching their X-ray crystal moduli. Most of the tensile moduli achieved for the crystalline polymers were 5–30% of the X-ray theoretical crystal modulus. Most attempts to produce high-performance polymers have failed due to low ductility. Therefore, it is notable that the tensile modulus achieved by PIN drawing of

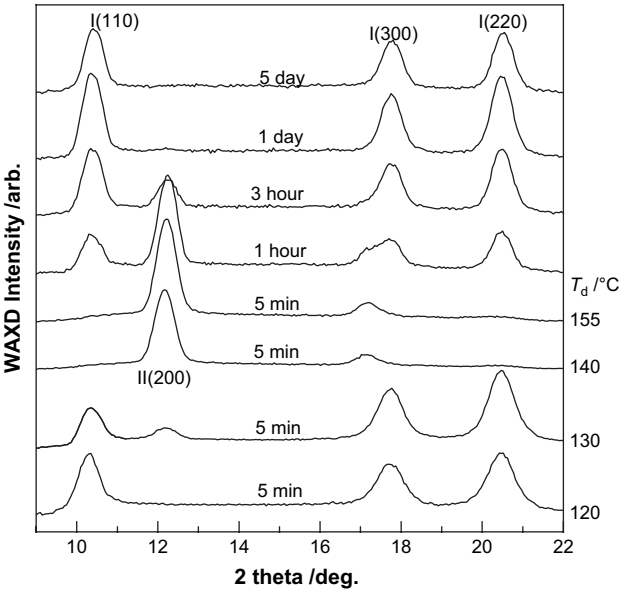

Fig. 8. WAXD equatorial diffraction profiles for a series of draw temperatures of DR = 10 samples left to stand for 5 min after PIN drawing and for a series of aged films with DR = 10 drawn at $T_d = 155$ °C.

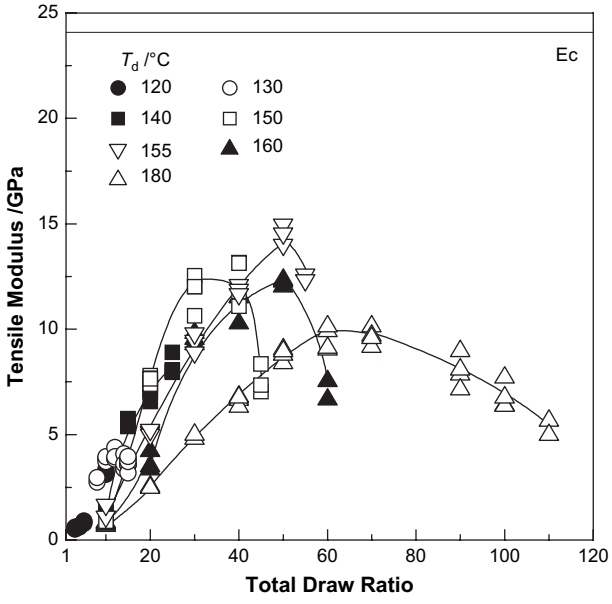

Fig. 9. Tensile modulus versus DR for PIN drawn samples.

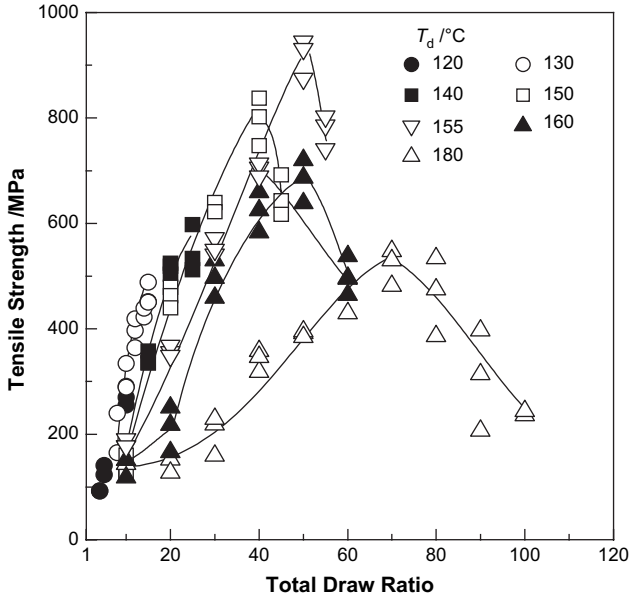

Fig. 10. Tensile strength versus DR for PIN drawn samples. The symbols are the same as in Fig. 9.

UHMW-PB1, which has low ductility in the crystalline state, corresponded to about 60% of the X-ray theoretical crystal modulus. From these results, the drawing method and draw conditions above T_m can be optimized to prepare high-performance polymers, even from polymers from which excellent mechanical properties could not be obtained previously.

Fig. 10 shows the tensile strength versus DR for the same sets of samples as shown in Fig. 9. The strength increased rapidly with DR in the lower DR region, reaching a maximum value of 300–900 MPa at higher DR, depending on the drawing temperature. The strength of drawn films increased rapidly with DR in all ranges of T_d, and the efficiency of the draw increased with decreasing T_d. Therefore, the strength at a given DR, as well as the modulus, was lower for the samples drawn at high T_d. The strength of the samples drawn at low T_d increased more rapidly with DR in the low DR region. However, the maximum achieved tensile strength of samples drawn at low T_d was significantly lower than that achieved for the highly drawn samples at high T_d, due to the markedly lower drawability of the former. The maximum strength of the drawn films was 900 MPa at DR = 50 and $T_d = 155$ °C. At even higher DR, the tensile strength decreased when the films were PIN drawn above T_m. The drop in the tensile strength at higher DR is probably also related to the formation of optical defect observed by OM (Fig. 11), as mentioned above in the discussion of tensile modulus versus DR.

The efficiency of draw was higher for samples drawn at lower T_d, based on f_c and tensile properties versus DR. The mechanical properties of the resultant samples drawn at a given DR were also higher for samples drawn at lower T_d, and the mechanical properties of the samples drawn at $T_d = 155$ °C were the highest, although the drawability was not the highest at $T_d = 155$ °C ($DR_{max} = 58$). Most likely, deformation of the entanglement networks in molten UHMW-PB1, which

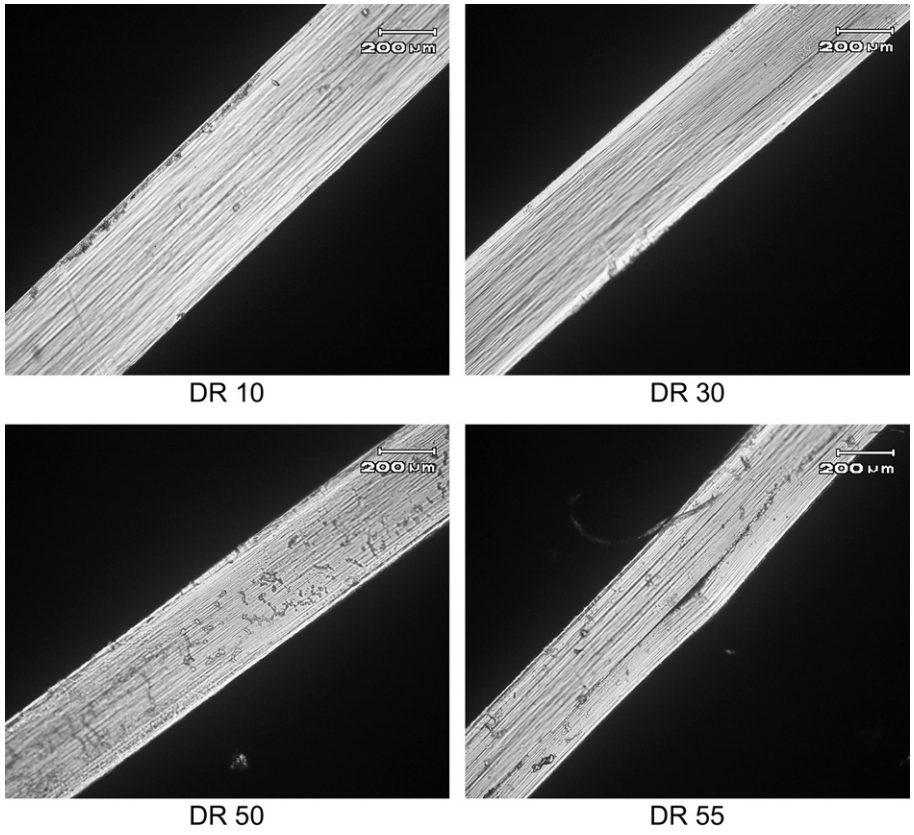

Fig. 11. Photomicrographs of MGC films with different DR values drawn at $T_d = 155$ °C. The photomicrographs were taken with crossed polarizers. Samples were oriented at an angle of 45° to the polarizers.

occurred during the PIN drawing, did not fully induce chain extension, orientation, and crystallization, depending on the drawing variables at high T_d.

Fig. 11 shows photomicrographs of the films at different DRs prepared by using the PIN drawing technique at $T_d = 155$ °C. Photomicrographs of the drawn films with DR = 10 and 30 show a highly aligned fibrous structure. However, in the highly drawn film with DR = 50, a number of dark and bright spots are noted within sample. Moreover, in the DR_{max} film (DR = 55), split lines were observed to run nearly parallel to the draw direction. They likely exist in the entire DR = 55 film. The decreases in tensile modulus and strength at higher DR were qualitatively in agreement with the appearance of the split along the fibrous axis. The split in the samples was possibly due to deterioration of the mechanical properties at higher DR at a given T_d. However, the chain orientation evaluated using f_c indicates nearly perfect chain orientation of the highly drawn film, even if a split occurs in the sample.

4. Conclusion

Melt-grown crystal films of UHMW-PB1 were ultradrawn using the PIN drawing technique in the temperature range of 30–220 °C. The drawability of MGC films was strongly affected by the initial sample thickness, the throughput rate, the contact time between the metal heater and the sample, and the PIN drawing temperature. The DR_{max} of the MGC films increased with increasing T_d and decreasing initial sample thickness and throughput rate. The drawability of the MGC films increased rapidly with T_d above about 130 °C, reaching a maximum at 200 °C, and then decreased sharply at higher temperatures. The rapid increase in ductility above 130 °C is ascribed to the decrease in the draw stress due to the onset of molecular motion above T_m (120–130 °C), which was detected by using DSC measurements. The highest DR of 170 was achieved by PIN drawing at $T_d = 200$ °C. The highest tensile modulus and strength of 14 GPa and 900 MPa, respectively, were achieved at $T_d = 155$ °C with DR = 50. Highly drawn samples had an extremely high chain orientation ($f_c = 0.996$), even for samples produced by melt drawing. These values are significantly higher than those achieved by drawing in the crystalline state, and the tensile modulus is the highest value yet reported, to the best of our knowledge. Further, the highest achieved modulus corresponded to 58% of the X-ray crystal modulus of isotactic PB1 (24 GPa). Ultradrawing above T_m of a polymer having low ductility in the crystalline state afforded ultradrawn films that had superior mechanical properties. The decrease in the modulus and strength at a higher DR were related to defects observed by OM.

References

[1] Luciani L, Sepälä J, Löfgren B. Prog Polym Sci 1988;13:37.
[2] Natta G, Corradini P, Bassi I. Nuovo Cimento Suppl 1960;15:52.
[3] Turner-Jones AJ. Polym Sci 1963;B18:455.
[4] Miller RL, Holland VF. Polym Lett 1964;2:519.
[5] Kopp S, Wittmann JC, Lotz B. Polymer 1994;35:908.
[6] Choi SY, Rakus JP, O'Toole JL. Polym Eng Sci 1966;6:349.
[7] Oda T, Maeda M, Hibi S, Watanabe S. Koubunshi Ronbunshu 1974; 31:129.
[8] Marigo A, Marega C, Cecchin G, Collina G, Ferrara G. Eur Polym J 2000;36:131.
[9] Gohil RH, Niles MJ, Petermann JJ. Macromol Sci Phys 1982;21: 3002.
[10] Goldbach G. Angew Makromol Chem 1973;29/30:213.
[11] Goldbach G. Angew Makromol Chem 1974;39:175.
[12] Nakafuku C, Miyaki T. Polymer 1983;24:141.
[13] Holland VF, Miller RL. J Appl Phys 1964;35:3241.
[14] Nakamura K, Aoike T, Usaka K, Kanamoto T. Macromolecules 1999; 32:4975.
[15] Smook J, Vos GJH, Doppert HL. J Appl Polym Sci 1990;41:105.
[16] Smith P, Lemstra PJ. Colloid Polym Sci 1981;259:1070.
[17] Kanamoto T, Porter RS. In: Lemstra PJ, Kleintjens LA, editors. Integration of fundamental polymer science and technology, vol. 3. London: Elsevier Appl. Sci.; 1989.
[18] Sawai D, Yamane A, Takahashi H, Kanamoto T, Ito M, Porter RS. J Polym Sci Polym Phys Ed 1998;36:629.
[19] Sawai D, Nagai K, Kubota M, Ohama T, Kanamoto T. J Polym Sci Polym Phys Ed 2006;44:153.
[20] Kanamoto T, Tsuruta A, Tanaka K, Takeda M, Porter RS. Macromolecules 1988;21:470.
[21] Zachariades AE, Porter RS. Strength and stiffness of polymers; plastic engineering series, vol. 4. New York: Marcel Dekker; 1983.
[22] Kanamoto T, Ohtsu O. Polym J 1988;20:179.
[23] Aharoni SM, Sibilia JP. J Appl Polym Sci 1979;23:133.
[24] Hu WG, Schmidt-Rohr K. Acta Polym 1999;50:271.
[25] Yamane A, Sawai D, Kameda T, Kanamoto T, Ito M, Porter RS. Macromolecules 1997;30:4170.
[26] Kanamoto T, Tsuruta A, Tanaka K, Takeda M, Porter RS. Polym J 1983;15:327.
[27] Sawai D, Watanabe D, Morooka N, Kuroki H, Kanamoto T. J Polym Sci Polym Phys Ed 2006;44:3369.
[28] Fujii S. Master Thesis, Tokyo University of Science, 1990.
[29] Tasaka S, Suzuki T, Miyata K. Koubunshi Ronbunshu 1982;39:127.
[30] Sakurada I, Kaji K. J Polym Sci 1970;C31:57.
[31] Endo R, Kanamoto T. J Polym Sci Polym Phys Ed 2001;39:1995.
[32] Uehara H, Nakae M, Kanamoto T, Zachariades AE, Porter RS. Macromolecules 1999;32:2761.
[33] Syoji M, Sawai D, Kanamoto T, Ohama T. Sen'i Gakkaishi 2004; 60:316.
[34] Samon JH, Schultz JM, Hsiao BS, Wu J, Khot S. J Polym Sci Polym Phys Ed 2000;38:1872.
[35] Wang J, Kuang X, Yan S. J Polym Sci Polym Phys Ed 2004;42:2703.
[36] Oda T, Maeda M, Hibi S, Watanabe S. Koubunshi Ronbunshu 1974; 31:291.
[37] Alexander LE. X-ray diffraction methods in polymer science. New York: John Wiley & Sons; 1969.
[38] Nishino T, Mukumoto M, Nakamae K. Polym Prepr Jpn 2001;50: 2782.